# An In-situ Sensor Technology for Simultaneous Spectrophotometric Measurements of Seawater Total Dissolved Inorganic Carbon and pH

Zhaohui Aleck Wang\*<sup>1</sup>, Frederick N. Sonnichsen<sup>2</sup>, Albert M. Bradley<sup>2</sup>, Katherine A. Hoering<sup>1</sup>

Thomas M. Lanagan<sup>2</sup>, Sophie N. Chu<sup>1</sup>, Terence R. Hammar<sup>2</sup>, and Richard Camilli<sup>2</sup>

<sup>1</sup> Department of Marine Chemistry and Geochemistry, Woods Hole Oceanographic Institution, McLean 203, MS # 8, 266 Woods Hole Road, Woods Hole, Massachusetts 02543, USA.

<sup>2</sup> Department of Applied Ocean Physics & Engineering, Woods Hole Oceanographic Institution, 266 Woods Hole Road, Woods Hole, Massachusetts 02543, USA.

## \*Corresponding author

Email: zawang@whoi.edu; Telephone: 1-508-289-3676; Fax: 1-508-457-2183

Keywords: dissolved inorganic carbon, pH, carbon dioxide, in-situ, sensor, ocean acidification, carbon cycle, spectrophotometry, seawater

#### ABSTRACT

1

2

3

4

5

6

7

8

9

10

11

12

13

14

15

16

17

18

19

20

21

22

23

A new, in-situ sensing system, Channelized Optical System (CHANOS), was recently developed to make high-resolution, simultaneous measurements of total dissolved inorganic carbon (DIC) and pH in seawater. Measurements made by this single, compact sensor can fully characterize the marine carbonate system. The system has a modular design to accommodate two independent, but similar measurement channels for DIC and pH. Both are based on spectrophotometric detection of hydrogen ion concentrations. The pH channel uses a flowthrough, sample-indicator mixing design to achieve near instantaneous measurements. The DIC channel adapts a recently developed spectrophotometric method to achieve flow-through CO<sub>2</sub> equilibration between an acidified sample and an indicator solution with a response time of only  $\sim$ 90s. During laboratory and in-situ testing, CHANOS achieved a precision of  $\pm 0.0010$  and  $\pm 2.5$ umol kg<sup>-1</sup> for pH and DIC, respectively. In-situ comparison tests indicated that the accuracies of the pH and DIC channels over a three-week time-series deployment were  $\pm 0.0024$  and  $\pm 4.1$  µmol kg<sup>-1</sup>, respectively. This study demonstrates that CHANOS can make in-situ, climatology-quality measurements by measuring two desirable CO<sub>2</sub> parameters, and is capable of resolving the CO<sub>2</sub> system in dynamic marine environments.

## INTRODUCTION

The marine carbon dioxide (CO<sub>2</sub>) system strongly influences the marine carbon cycle. It helps regulate the Earth's climate by controlling the amount of CO<sub>2</sub> that exchanges between the ocean and the atmosphere. Currently, the ocean absorbs about one quarter to one third of the anthropogenic CO<sub>2</sub> released to the atmosphere <sup>1-3</sup>, therefore reducing the rate of atmospheric CO<sub>2</sub> increase and curbing global warming. However, oceanic uptake of anthropogenic carbon is causing a rapid change in seawater carbonate chemistry, a phenomena referred to as ocean

acidification. In ocean acidification, excess CO<sub>2</sub> lowers seawater pH, increases total CO<sub>2</sub> concentration, and decreases calcium carbonate saturation <sup>4-5</sup>. Changes in the marine CO<sub>2</sub> system may result in complicated responses and feedbacks in the ocean including changes in the marine carbon and other elemental cycles, as well as changes in marine biology and ecology <sup>4,6-7</sup>. Ocean acidification also reduces seawater buffering capacity, which slows oceanic carbon uptake and acts as a positive feedback in the increase of atmospheric CO<sub>2</sub> <sup>3,8</sup>.

Precise and accurate characterization of the marine CO<sub>2</sub> system is critical to studying the marine carbon cycle and ocean acidification. The development of in-situ sensor technologies for CO<sub>2</sub> parameters have been widely recognized as a research priority in the carbon and ocean acidification research communities <sup>9-14</sup>. It is important to study dynamics of the marine CO<sub>2</sub> system on various time scales ranging from minutes to decades, and spatial scales of meters to kilometers. Because of the high costs associated with traditional bottle sampling, it is more effective to use autonomous sensors and instruments to achieve high-resolution data <sup>15</sup>.

The marine CO<sub>2</sub> system is described by four measurable, primary parameters: total dissolved inorganic carbon (DIC), partial pressure of CO<sub>2</sub> (pCO<sub>2</sub>) or CO<sub>2</sub> fugacity (fCO<sub>2</sub>), pH, and total alkalinity (TA). Measurements of any two of the four parameters are required to calculate the others and fully resolve the carbonate system using seawater acid-base equilibria. Simultaneous measurements of two CO<sub>2</sub> parameters are thus attractive. However, different measurement pairs will generate a range of calculation errors as a result of analytical errors, uncertainties in equilibrium constants, and their non-linear propagation in the calculations. Large errors result when pCO<sub>2</sub> and pH are used due to their strong co-variation <sup>16</sup>. The errors are often minimized when DIC and pH, or DIC and pCO<sub>2</sub> are used <sup>9</sup>. However, only in-situ pCO<sub>2</sub> and pH

sensors are commonly available <sup>17-21</sup>. In contrast, in-situ DIC sensor technologies are much less mature but are highly desirable <sup>9</sup>.

Spectrophotometric methods are advantageous for simultaneous measurements of CO<sub>2</sub> system parameters because all of the measurements can be made by absorbance detection of a pH sensitive sulfonephthalein indicator in either the water sample or a standard solution <sup>22</sup>. Moreover, spectrophotometric measurements are highly sensitive and stable, making them well-suited for in-situ, underwater deployments. In addition, this method uses a low amount of sample and reagent, requires low power consumption, and makes direct measurements of seawater. The spectrophotometric method has become the benchmark for high-accuracy seawater pH measurements <sup>15</sup>. In this method <sup>15, 23</sup>, a small amount of pH indicator is added to the sample water and the pH is determined by measuring the ratio of the absorbance maxima of the indicator's acid and base wavelengths. In-situ applications of this method have achieved a measurement uncertainty of 0.001-0.003 <sup>18-19</sup>, and are relatively immune to instrument drift often encountered by potentiometric pH measurements.

In-situ DIC sensors for seawater applications have recently been developed based on CO<sub>2</sub> equilibration between an acidified sample and a standard solution followed by either spectrophotometric or conductometric detection <sup>24-25</sup> (Table S1). Other DIC sensors, based on gas-sample CO<sub>2</sub> equilibration followed by infrared detection, are also under development. The established spectrophotometric DIC method <sup>22, 24, 26</sup> uses a piece of Teflon AF 2400 (DuPont<sup>TM</sup> copolymer) capillary tubing as both an optical cell and a CO<sub>2</sub> equilibrator since the material is highly permeable to CO<sub>2</sub> molecules and can act as a liquid-core waveguide (LCW) for optical detection. The spectrophotometric detection occurs after full CO<sub>2</sub> equilibration is established between the acidified sample and the indicator solution. The time-limiting step of this method is

the time that it takes for CO<sub>2</sub> to equilibrate across the Teflon AF 2400 tubing, which is about 5 minutes. An improved spectrophotometric DIC method <sup>27</sup> was recently developed to achieve a faster response time and to allow for near continuous detection using a dynamic equilibration and a countercurrent flow design (Figure 1). The response time of this method varies with indicator flow rates, but can be as fast as 22s if partial equilibration<sup>27</sup> is used. The improved method also overcomes optical signal drifting that can occur when Teflon AF tubing is used as the optical cell.

This paper will describe the development and testing of a new, in-situ carbon sensor, Channelized Optical System (CHANOS), which uses a modular design that is capable of making simultaneous spectrophotometric measurements of seawater DIC and pH. The DIC channel uses the improved spectrophotometric method <sup>27</sup>. The sensor design was targeted for high-resolution, time-series measurements at a fixed location. CHANOS is one of the first systems that is able to fully resolve the carbonate system with a desirable pair of CO<sub>2</sub> system parameters in a single system. CHANOS has a built-in mechanism for in-situ calibration, which ensures high quality measurements throughout a deployment cycle and reduces the need for laboratory calibration. Insitu tests indicate that the system is able to make high-resolution, climatology-quality measurements <sup>15</sup> to resolve seawater CO<sub>2</sub> system dynamics.

## METHODS AND MATERIALS

# Principles.

(1) pH – The CHANOS pH channel uses a flow-through design in which seawater directly and continuously mixes with an indicator solution <sup>22</sup>. It is based on the well-established spectrophotometric pH method <sup>15, 23</sup>, where dissociation of the added sulfonephthalein indicator

(H₂I) in seawater is dominated by HI⁻ ← K₁ → H⁺ + I²⁻; K₁ is the dissociation constant of the
 indicator acid species HI⁻. Combining Beer's Law, seawater pH can then be expressed as:

$$pH = pK_1 + log \frac{R - e_1}{e_2 - Re_3},$$
 (1)

where  $R = \frac{1}{\lambda_2} A/\frac{1}{\lambda_1} A$ , and  $\lambda_1$  and  $\lambda_2$  are the wavelengths for the absorbance maxima of HI<sup>-</sup> and I<sup>2-</sup>;

 $e_1$ ,  $e_2$ , and  $e_3$  are indicator molar absorbance ratios at wavelengths  $\lambda_1$  and  $\lambda_2$ :

$$e_1 = \frac{\lambda_2 \in_{\text{HI}}}{\lambda_1 \in_{\text{HI}}}, \quad e_2 = \frac{\lambda_2 \in_{\text{I}}}{\lambda_1 \in_{\text{HI}}}, \quad e_3 = \frac{\lambda_1 \in_{\text{I}}}{\lambda_1 \in_{\text{HI}}}, \tag{2}$$

where  $_{\lambda_1} \in_{I}$  and  $_{\lambda_2} \in_{I}$  are the molar absorbances of  $I^{2-}$  at wavelengths  $\lambda_1$  and  $\lambda_2$ , and  $_{\lambda_1} \in_{HI}$  and  $_{\lambda_2} \in_{HI}$  refer to the molar absorbances of HI at wavelengths  $\lambda_1$  and  $\lambda_2$ . The indicators used in this work included thymol blue sodium salt  $^{28}$  ( $\lambda_1 = 435$  nm and  $\lambda_2 = 596$  nm) and m-cresol purple sodium salt  $^{29}$  ( $\lambda_1 = 434$  nm and  $\lambda_2 = 578$  nm). A non-absorbing wavelength (700 nm) was used to correct baseline changes. Calibrations of pK<sub>I</sub>,  $e_1$ ,  $e_2$ , and  $e_3$  of the two indicators for typical seawater temperature and salinity have been established in laboratory experiments  $^{28-29}$ . It has been demonstrated that in-situ spectrophotometric pH measurements require infrequent or no calibration  $^{19,22}$ .

(2) DIC – The CHANOS DIC channel utilizes continuous, countercurrent flow between the indicator and acidified sample (Figure 1), instead of CO<sub>2</sub> equilibration with static indicator used in the previous method <sup>24, 26</sup>. This dramatically improves CO<sub>2</sub> equilibration efficiency by maintaining a chemical concentration gradient <sup>30-32</sup> across the wall of the gas-permeable Teflon AF capillary tubing <sup>27</sup>. CO<sub>2</sub> fugacity (fCO<sub>2</sub>) in the indicator equilibrates with fCO<sub>2</sub> in the acidified sample as the indicator flows through the Teflon AF tubing that is enclosed in the

sample flow cell. Partial or full CO<sub>2</sub> equilibration can be achieved depending on the indicator flow rate. After equilibration, DIC (as total CO<sub>2</sub>) of the acidified sample (denoted by subscript *a*) is proportional to *f*CO<sub>2</sub> of the internal indicator solution (denoted by subscript *i*) <sup>27</sup>:

$$\log(p \times fCO_2)_a = \log(p \times \frac{[DIC]}{(K_0)_a}) = \log(fCO_2)_i$$
(3)

 $(K_0)_a$  is the Henry's Law constant <sup>33</sup> for the acidified sample; p (value 0-1) is the exchange efficiency or percentage of equilibration of CO<sub>2</sub> when the indicator exits the Teflon tubing. If the indicator reaches full CO<sub>2</sub> equilibration, p has a value of 1 or 100%. Partial equilibration (p<1) can be achieved if a faster response time is desired <sup>27</sup>. The response time for the flow-through method refers to the time required to obtain a stable reading for detection, not CO<sub>2</sub> equilibration time inside the Teflon AF tubing <sup>27</sup>, while in the previous method <sup>22, 24</sup>, they are the same. The indicator solution can reach 100% CO<sub>2</sub> equilibration within 70s once it travels through the Teflon tubing <sup>27</sup>. To ensure full equilibration, a travel time of ~2 minutes was used for this study (see explanation in Results and Discussion). Essentially, each measured data point under the continuous flow-through detection represents a running average of the flow-through sample over the indicator travel time in the Teflon AF tubing.

The indicator is dissolved in a sodium carbonate solution with a known TA. Based on acidbase equilibrium equations and Beer's Law, when it fully equilibrates with CO<sub>2</sub> across the Teflon AF tubing after sample acidification (p = 1), Eq. 3 becomes <sup>26-27</sup>:

$$\log \frac{[DIC]}{(K_{\theta})_a} = B(t) - \log(K_{\theta})_i - \log \left(\frac{R - e_1}{1 - Re_3 / e_2}\right)$$
(4)

 $(K_{\theta})_i$  is the Henry's Law constant <sup>33</sup> for the internal indicator solution. B(t) is determined by the solution composition <sup>24, 26</sup>:

$$B(t) = \log(TA + [H^+] - [I^{2-}])_i + \log\left(\frac{K_i e_2}{K_1}\right)_i$$
 (5)

130

131

132

133

134

135

136

137

138

139

140

141

142

143

144

145

146

147

148

149

 $K_1$ ' is the carbonic acid first dissociation constant for the internal solution. Bromocresol purple (BCP) was used as the DIC indicator, where  $\lambda_1 = 432$  nm and  $\lambda_2 = 589$  nm. Baseline drift correction was conducted similarly to pH drift corrections. Except for B(t), the values for all of the constants and coefficients in Eqs. 3-5 were previously determined  $^{26-27, 34}$ . A 1-cm optical cell was used to make the sensor more compact. With a shorter cell, the use of a higher BCP (~20 μM) and lower TA (~800 μmol kg<sup>-1</sup>) concentration as compared to the previous study (10 cm cell, ~2 µM BCP, and ~1000 µmol kg<sup>-1</sup> TA) <sup>26</sup> allows for good absorbance measurements. Use of a lower indicator concentration solution with a 10 cm optical cell in the previous study allows for a wider DIC range  $(1000 - 3000 \, \mu \text{mol kg}^{-1})$  wherein B(t) can be considered a constant at a given temperature. By making adjustments to the indictor for use with a shorter optical cell for this study, it was still sufficient to treat B(t) as a constant for seawater with a DIC range of 1700 – 2200 μmol kg<sup>-1</sup>, which covers many marine applications, including our field test. This is because the  $TA + [H^+] - [I^{2-}]$  term in Eq. 5 only varies by 0.07% from a value of 797.2 µmol kg<sup>-1</sup> <sup>1</sup> in the range of 796.6 - 797.7 umol kg<sup>-1</sup>. Such variability is below the detection limit of the current sensor ( $\sim 0.10\%$ ). B(t) can thus be experimentally calibrated over the range of temperature encountered in nature using Certified Reference Material (CRM) obtained from A.G. Dickson at Scripps Institution of Oceanography. CHANOS. CHANOS consists of four major components: two junction boxes (J-boxes), one for pH and one for DIC, a pressure housing, 4 custom-made stepper-motor syringe pumps, and a Seabird pump (Model 5P) (Figure 2). Each J-box contains one 2-port and one 3-port

solenoid valve (161K011, T161PK031, NResearch Inc.), a sample diaphragm pump (NF5, KNF

Group International), thermistors, and optical and fluid handling components (Figure 3). J-box components are described in Supporting Information.

The pressure housing contains all of the controlling electronics, light sources, and the optical detection system. The controlling software runs on TERN microprocessors (see details in Supporting Information).

Four custom-made syringe pumps were made using high precision stepper motors (Phytron, Model ZSS 25-GPL26; see Supporting Information). A Seabird pump is used to pump sample water through a coarse copper mesh filter (mesh size  $100~\mu m$ ), and each channel then subsamples water through an additional copper mesh filter (mesh size  $40\mu m$ ) to reduce fouling within the system. Discrete bottle measurements confirmed that there was no detectible difference between mesh-filtered and non-filtered samples for local coastal waters (mean difference  $1.6\pm3.5~\mu mol~kg^{-1}$ , n=9).

CHANOS runs on repeatable cycles, which include a series of mission steps for both channels (Figure S1). For the DIC measurement cycle, measurement preparation steps include filling the acid, reference, and indicator syringes, flushing the acidified sample and reference, and recording a reference spectrum (Figure S1). Thereafter, indicator flows continuously through the Z-cell while acid continuously mixes with sample water and flows through the sample line until the indicator and acid syringes are emptied. Stable readings are achieved after the indicator has flowed for ~90s. Thereafter, the system records ~6 minutes of spectra with near continuous DIC measurements (~12s per measurement). Changes in the measurement cycle and size of the syringes can allow for higher resolution measurements (see Supporting Information). The cycle is similar for in-situ calibration, except that CRM is used in place of an external sample (Figure 3A). For the pH channel, similar preparation steps take place before near continuous

measurements (every ~12s for ~8 minutes) commence (Figure S1). At a pre-determined interval of every few days, the pH channel is flushed with a Triton 100 detergent solution for cleaning purposes. For both channels, all steps are customizable depending on deployment purposes.

Reagent. BCP sodium salt (Sigma-Aldrich) was used to make 4 mM indicator stock solution that was stored in opaque glass bottles. Working BCP solutions of ~20 μM were prepared using the indicator stock solution in sodium carbonate (Na<sub>2</sub>CO<sub>3</sub>) solution (Extra-pure, Acros Organics) <sup>27</sup>. Final alkalinity of the working solutions were ~800 μmol kg<sup>-1</sup>, which was chosen so that the pH of the final CO<sub>2</sub>-equilibrated indicator for typical seawater DIC concentrations (1700 – 2200 μmol kg<sup>-1</sup>) fall within the range of ~5.6 – 6.4, where indicator absorbance change is sensitive <sup>26</sup>. For each liter of working indicator solution, 0.5 ml of 2.8% lauryl sulfate sodium salt solution was added to serve as a surfactant for cleaning purposes. Reference solutions had identical composition as that of the indicator solutions, but did not have indicator. Gas-impermeable laminated bags (Calibrated Instruments, Inc.) were used to store the working indicator and reference solutions. In-situ tests indicated that the bagged indicator solution did not have any appreciable changes during the three-week field test (Figure S2). Hydrochloric acid, used to acidify the DIC samples (HCl, 2.5M) at a sample-to-acid mixing ratio of ~800:1 <sup>22</sup>, was stored in intravenous bags (HyClone Latainer BPC, Thermo Scientific).

For the pH channel, thymol blue (TB) sodium salt (Sigma-Aldrich, ACS Certified) was used to make working indicator solutions with concentrations between 1.5-2.0 mM. TB is well suited for pH  $\geq 7.9^{28}$  which is often observed in the local waters where the deployment occurred. The R ratio of the indicator solution was adjusted (R $\sim$ 0.77) to minimize indicator-induced pH perturbations. The pH indicator solution was also stored in a laminated bag. The sample-to-indicator mixing ratio was maintained at  $\sim$ 700:1, so that the final indicator concentration was  $\sim$ 2

 $-3 \mu M$ . The indicator perturbation was generally smaller than  $\pm 0.002$ , and was corrected based on the standard procedure  $^{15}$ . pH measurements were also corrected for the impurity of the indicators based on the recommended method through comparison with purified m-cresol purple (mCP) sodium salt  $^{29}$ .

Calibration. Each batch of DIC indicator (BCP) solution was calibrated using CRMs to obtain the calibration constant B(t) (Eq. 5)  $^{22, 24}$ . In addition to lab calibration, in-situ calibration was conducted autonomously using a solenoid valve to switch between sample water and CRM (Figure 3A), which was also stored in a laminated bag. Measurements by CHANOS indicate that there was no apparent change in DIC concentration of the bagged CRM from the certified CRM value over the three-week field test (Figure S2;  $\Delta$ DIC =  $0.3\pm2.1$  µmol kg<sup>-1</sup>, n = 5). A laboratory test also suggests that when CRM is carefully bagged, differences in DIC concentration between bags is small ( $\Delta$ DIC =  $0.3\pm0.8$  µmol kg<sup>-1</sup>, n = 4) and no detectible DIC changes relative to the certified CRM value occurred in the bagged CRM over four weeks (Figure S3). The B(t) temperature function was calibrated in the lab by making a set of measurements over a range of sample temperatures controlled by a thermostated water bath  $^{22, 24}$ . This temperature function was also determined in-situ using the natural variability of seawater temperature and CRM during the field deployment. All previously calibrated constants for spectrophotometric pH measurements  $^{15, 28-29}$  (Eqs. 1 – 2) can be used for CHANOS pH calculations.

In-situ Testing and Groundtruthing. CHANOS was tested in-situ for several months in Fall 2013 at the Iselin dock of the Woods Hole Oceanographic Institution (WHOI), Woods Hole, MA, USA. The first several weeks were used to diagnose the overall functionality of the instrument and to make necessary changes. Thereafter, in-situ measurements were made for three weeks. The sensor was programed to make measurements every 40 minutes (Figure S1).

Although such a long wait time between measurements is not sufficient for capturing short time scale variability, it was sufficient for field testing.

The sensor, contained in a Pelican case, was hung in a testing well at ~5m depth. The case provided protection to the sensor and reduced system fouling. A Seabird conductivity-temperature-depth (CTD) sensor (SBE 49) was also deployed with the sensor. A piece of Tygon tubing used for discrete sampling was co-located with the sensor sample intake for direct comparison. A field peristaltic pump was used to pump water onto the dock to collect discrete DIC and pH samples in order to assess sensor accuracy. Bottle samples were collected in 250 mL borosilicate glass bottles and poisoned with mercuric chloride following the standard procedure <sup>15</sup>. Their measurements are described in Supporting Information.

#### **RESULTS AND DISCUSSION**

pH Channel. The CHANOS pH channel has similar measurement characteristics as previously developed spectrophotometric pH sensors<sup>18-19</sup>. The flow-through design allows for continuous pH measurements after taking reference spectra. The syringe pumps allow for precise delivery and therefore maintain a stable sample-to-indicator mixing ratio during long deployments. They also minimize indicator consumption. The self-cleaning mechanism for the pH sample line using detergent (Figure 3b) effectively reduces fouling inside the sample tubing and maintains throughput light in the pH optical cell. During the three week in-situ testing, the light level was only reduced by ~10%.

Sensor performance was evaluated in the laboratory and during the field deployment. During laboratory experiments, spectra (n = 15) recorded within a pH measurement cycle had a precision of  $\pm 0.0010$  pH units (data not shown). Across measurement cycles (n = 10) of the same sample, the CHANOS pH channel also achieved a precision (repeatability) of  $\pm 0.0010$  pH units

which is comparable to similar pH sensors  $^{19, 22}$ . During the three-week field deployment, the precision of the pH measurements was  $\pm 0.0019$  pH units (n = 13) (Figure 4) over repeated measurements during the last two minutes of a measurement cycle. This standard deviation is slightly larger than that found in the laboratory experiments, which suggests that there may be high variability in water chemistry at the testing site over a short time period. Overall, CHANOS showed good in-situ pH repeatability.

DIC Channel. The response time for CHANOS DIC measurements was at least 3 times faster than previous spectrophotometric measurements using a similar size of Teflon AF 2400 tubing <sup>22, 24, 26-27</sup>. At the current settings, it takes ~90s for fresh indicator solution to achieve a stable reading at 100% equilibration for samples with a DIC concentration of ~2000 μmol kg<sup>-1</sup> (Figure 5), compared to about 300s in the previous development <sup>22, 24</sup>. Temperature had an insignificant influence on the response time for the current design based on lab experiments (Figure 5). Such insensitivity is expected as the response time herein reflects the time that it takes for the system to flush the indicator line with newly CO<sub>2</sub> equilibrated solution, which is not temperature dependent.

Currently, CHANOS makes DIC measurements using flow-through, full CO<sub>2</sub> equilibration and requires only calibration of a single operation constant B(t) (Eq. 5). The DIC measurement precision is  $\pm 2.5$  µmol kg<sup>-1</sup> as determined by repeated measurements, which is similar to previous underway and in-situ systems  $^{22, 24-25}$  (Table S1).

Calibration constant B(t) is a function of temperature as described by Eq. 5, where  $K_I$ ,  $e_2$ , and  $K_I$ ' of the indicator solution are all temperature dependent (Figure 6A)  $^{22, 24, 26}$ . In theory, B(t) can be calculated using the knowledge of the indicator solution composition and thermodynamic constants via Eq. 5. However, the terms in Eq. 5 may have an overall uncertainty

that exceeds the acceptable range for climatology-quality DIC measurements. The B(t)-temperature function was thus experimentally determined by measuring CRMs at different temperatures. Such a strategy is convenient as it does not require knowledge of all terms in Eq. 5, but results in well-constrained uncertainties in DIC measurements. The mean difference in B(t) between measured and predicted values based on the best-fit curve in Figure 6A can be translated to a DIC error of  $0.4\pm2.7~\mu\text{mol}~\text{kg}^{-1}$ , which is similar to the uncertainty in repeated measurements.

265

266

267

268

269

270

271

272

273

274

275

276

277

278

279

280

281

282

283

284

285

286

287

The CHANOS in-situ calibration routine using CRMs allows for the determination of the B(t)-temperature function under real deployment conditions. Figure 6B shows the B(t)temperature curve obtained during the deployment of CHANOS in November 2013 at the WHOI Iselin dock. The in-situ calibration was conducted every 48 to 72 hours. The uncertainty in B(t)relative to the best-fit line in Figure 6B was equivalent to a DIC error of 0.1±4.9 µmol kg<sup>-1</sup>. The larger uncertainty for the in-situ calibration as compared to that obtained under laboratory conditions (Figure 6A vs. 6B) is largely due to one data point near 1/T of 0.00351 (t = 11.6 °C; circled data point in Figure 6B). Without it, the best-fit curve has a R<sup>2</sup> value of 0.9980, equivalent to a DIC error of 1.6±2.7 µmol kg<sup>-1</sup>, comparable to that determined in the lab experiment. The cause of this apparent 'outlier' is unknown. Given the stableness of CRM measurements during the deployment (Figure S2) and good CRM storage in aluminum bags (Figure S3), in-situ calibration of B(t) should provide a valid means for gauging sensor consistency and performance. The coefficients of the quadratic curves between Figure 6A and 6B showed large differences. This might be due to the temperature dependence of the spectrophotometer and the light, which operated at different temperatures in Figures 6A (room temperature) and 6B (in-situ temperature). Further testing will be conducted to determine the In-situ Groundtruthing. During deployment at the WHOI Iselin dock, CHANOS measurements were directly compared with discrete sample measurements (Figures 7-8). The DIC channel generated more measurement data than the pH channel because the pH sample pump malfunctioned during the first week of measurement testing. During the deployment, the DIC concentration ranged from 1864 to 2012  $\mu$ mol kg<sup>-1</sup>, and pH in the total scale (pH<sub>T</sub>) varied from 8.029 to 8.118 (Figure 7). Meanwhile, salinity only showed a small variation (32.2 – 32.7), and water temperature exhibited a general cooling trend of ~4.5°C. The diurnal pattern of salinity was often irregular suggesting that the hydrology may not mainly be controlled by the tide. There was a somewhat significant negative correlation between pH<sub>T</sub> and temperature (pH<sub>T</sub> = -0.0147t + 8.2046, R<sup>2</sup> = 0.7034, n=320), while DIC was not conservative relative to salinity. These observations suggest that in addition to temperature, biogeochemical processing and physical mixing may also have affected carbonate chemistry at the site.

CHANOS showed good agreement with discrete samples. The mean difference between CHANOS and discrete DIC samples was 0.8±5.2 μmol kg<sup>-1</sup> (n=15, Figure 8). The mean absolute difference was 4.1±2.9 μmol kg<sup>-1</sup>. Part of this difference may be due to discrete sampling and analytical errors of the DIC bottle samples (~2.0 μmol kg<sup>-1</sup>), and the rest is comparable to the precision of CHANOS (±2.5 μmol kg<sup>-1</sup>). For pH, the mean difference between the sensor and discrete measurements was -0.0010±0.0033 pH units (n = 13) with a mean absolute difference of 0.0024±0.0023 pH units (Figure 8). Such a performance is comparable to existing in-situ spectrophotometric sensors (http://www.sunburstsensors.com) <sup>18-19</sup>. Overall, CHANOS achieved the development goal, which was to make climatology-quality, simultaneous, in-situ measurements of two primary CO<sub>2</sub> parameters – DIC and pH. The deployment data (Figure 7)

also indicate that the new sensor is capable of resolving the high variability of the carbonate system in dynamic environments.

311

312

313

314

315

316

317

318

319

320

321

322

323

324

325

326

327

328

329

330

331

332

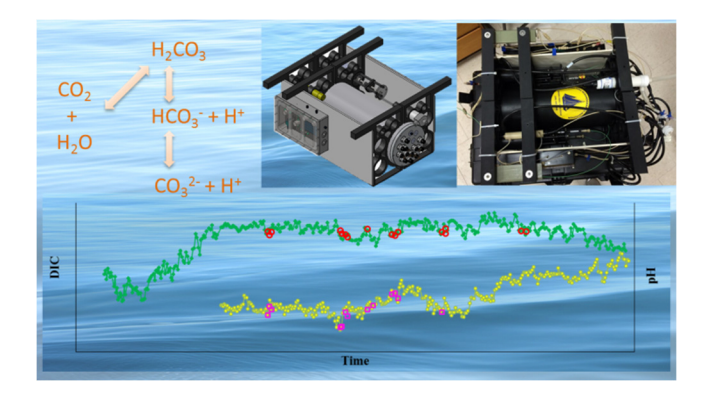
333

Implication and Future Development. Built in, in-situ DIC calibration for CHANOS has the advantage for remote deployment where discrete sampling and measurements to evaluate sensor performance is difficult. The November 2013 test data suggests that in-situ calibration during the deployment is sufficient rather than taking discrete bottle samples to calibrate the system. This includes calibrating the B(t) constant with respect to temperature for all new reagents (Figure 6B). Storage of CRM and DIC indicator are also the key to successful deployments. Although not found in this deployment, DIC and TA changes in bagged CRM and changes in TA of DIC indicator solutions have occurred in the past. TA of the indicator and CRM may both change if certain layers of the multi-layered storage bags deteriorate, causing the aluminum layer to come in direct contact with the solution, or if mercury-resistant biological contamination occurs. Changes in solution DIC in bags due to CO2 exchange have been observed less frequently. Improved methods for long-term storage of CRM and indicators are being studied. If the storage is robust, in-situ calibration will reduce the need for laboratory calibration, which adds convenience for sensor deployment. Alternatively, instead of using CRM, another calibrated indicator solution can be used during deployment to cross-check the stability of the primary indicator solution and to gauge measurement quality.

Although both the pH and DIC methods allow for near continuous measurements, CHANOS has not been fully tested for such a capability. The current syringe pumps cannot achieve such measurements for a long period of time, as they require a few minutes of refill after a complete stroke. Such a waiting time is insignificant for time-series deployments. Future development will target high-resolution measurements required for other deployment platforms,

such as CTD profilers and autonomous underwater vehicles, where any delay time will matter. For these fast-moving platforms, one can take full advantage of the flow-through CO<sub>2</sub> equilibration method <sup>27</sup>.

Future work will also target longer deployments with groundtruthing in marine ecosystems of different biogeochemical conditions to demonstrate long-term robustness of the sensor. The modular design of CHANOS adds flexibility for future development for measurements of other parameters. Because of the similarity between spectrophotometric DIC and pCO2 measurements, with minor modification, pCO2 can be measured with one of the CHANOS channels using a different indicator <sup>22,35</sup>. The main difference is that the sample will not be acidified. With further development, TA could also be measured using an improved method for single-point spectrophotometric titration <sup>36</sup>. The future goal is to further develop the sensor to make simultaneous measurements of any combination pair of the four primary carbonate parameters in order to meet a wide range of deployment goals. This study has demonstrated that the development of CHANOS has achieved its first milestone.



# **TOC/Abstract Art**

## **FIGURES**

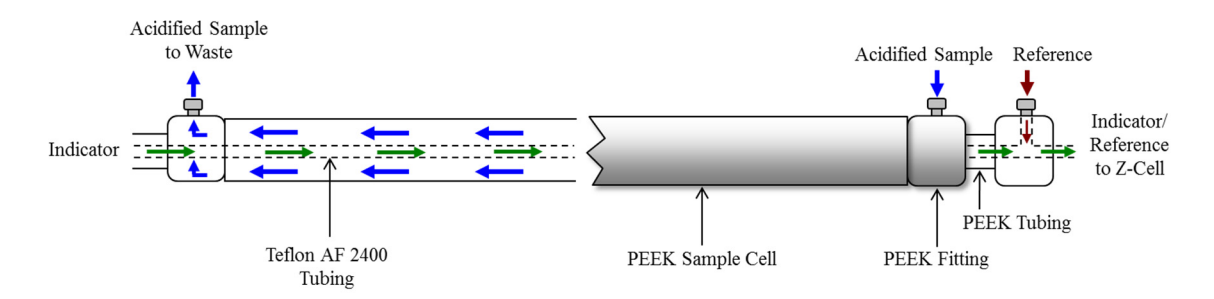


Figure 1. Schematic drawing of the DIC equilibration cell with the countercurrent flow design.

Blue and green arrows indicate acidified sample and indicator solution flow, respectively.

Reference solution (red arrows) bypasses the equilibration cell and directly enters the optical Z-

358 cell.

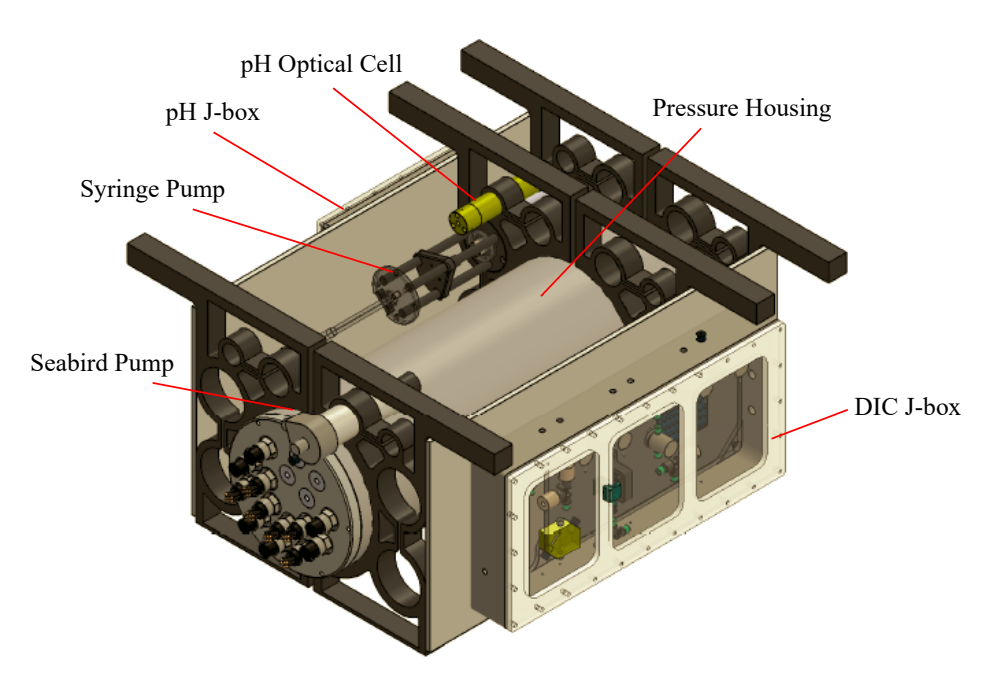
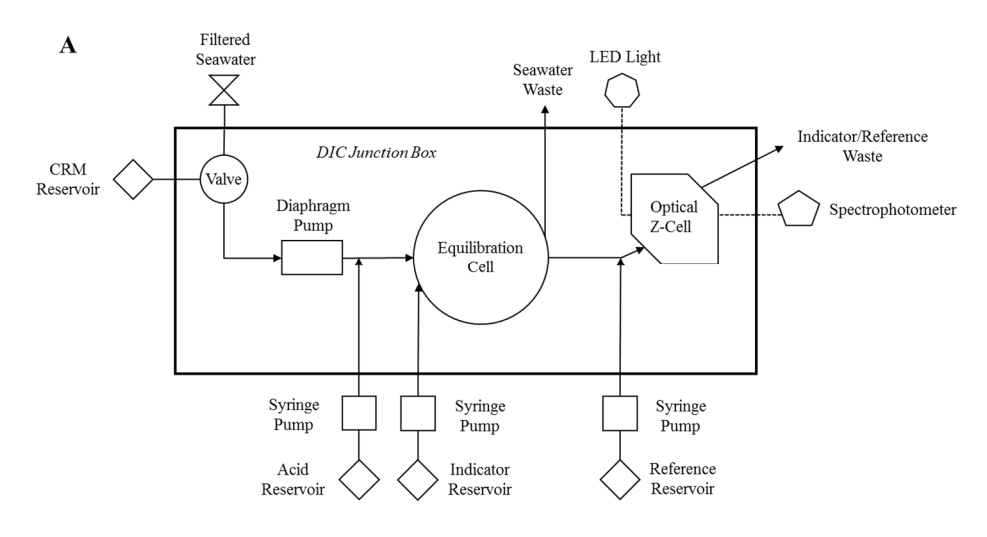


Figure 2. Schematic drawing of CHANOS for spectrophotometric DIC and pH measurements.



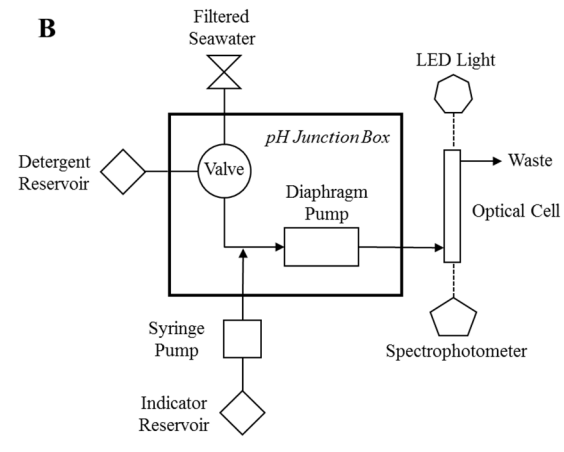


Figure 3. Schematic drawings of DIC (A) and pH (B) channels of the CHANOS.

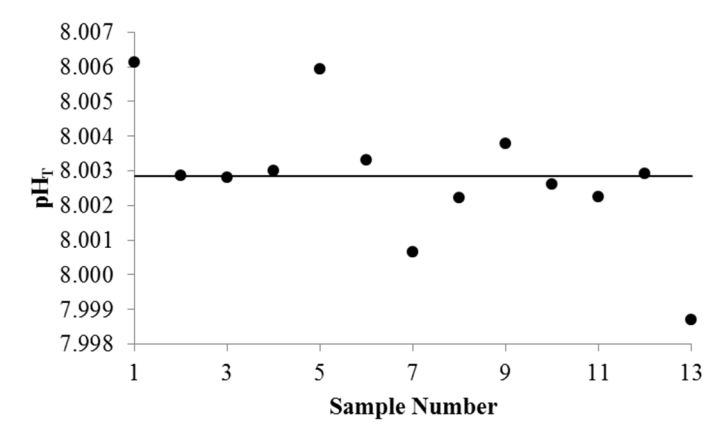


Figure 4. In-situ, repeated measurements of coastal waters at the WHOI Iselin dock in November 2013. The measurements were made over  $\sim$ 2 minutes, with a pH of  $8.0029\pm0.0019$  (n = 13), a temperature of  $10.2\pm0.1$  °C and a salinity of  $32.5\pm0.1$ .

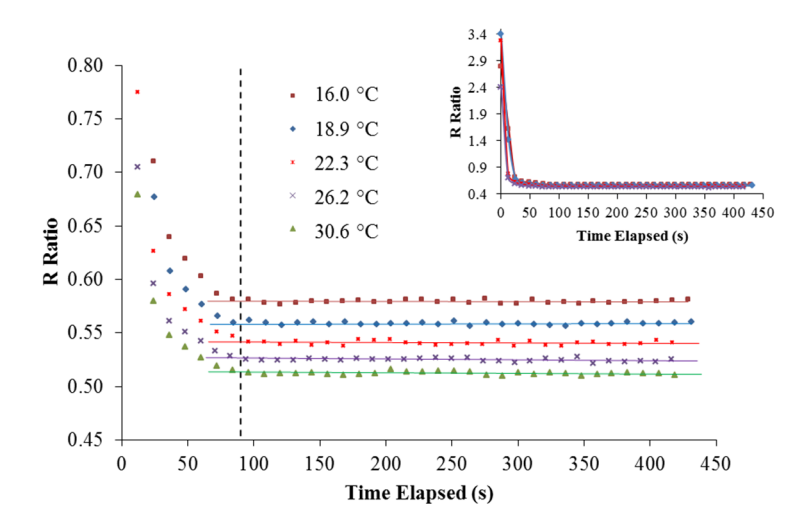


Figure 5. Response time of DIC measurements by the CHANOS sensor at different temperatures. The DIC sample has a concentration of  $2035.9\pm1.9~\mu\text{mol kg}^{-1}$ . The inset shows all of the experimental data. Color lines are best-fit lines corresponding to the data from each temperature after a time elapsed of 150s. These lines are extended for better viewing. The vertical dotted line represents the 90s mark, after which all data points at a given temperature varied with a standard deviation  $<\pm0.0014$  relative to the best-fit lines.

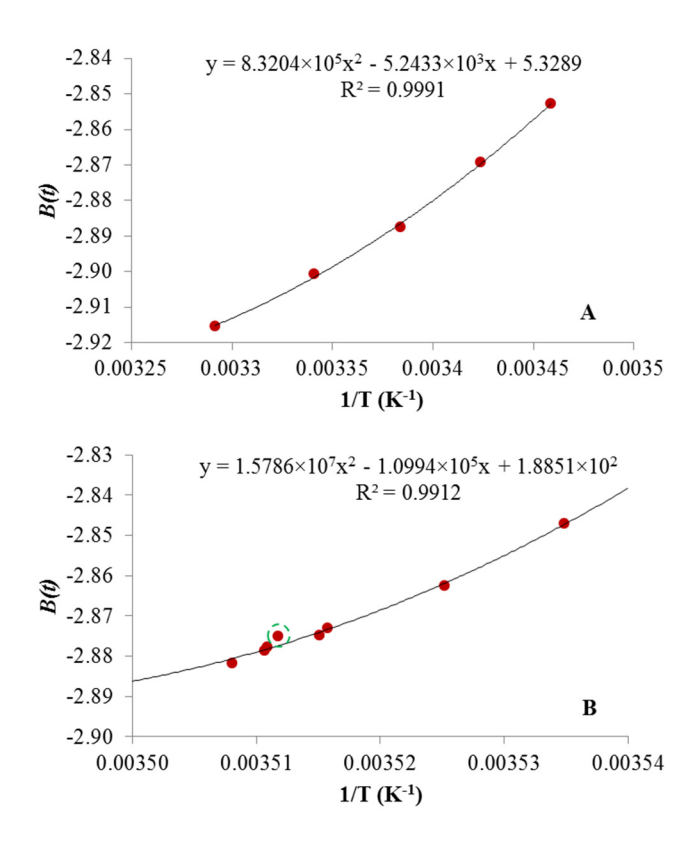


Figure 6. DIC calibration constant B(t) as a function of measurement temperature under (A) laboratory conditions (t = 15.9 – 30.6°C) and (B) in-situ conditions (t = 9.7 – 11.9°C). Different indicator solutions were used in (A) and (B). The solid lines are  $2^{nd}$  degree polynomial best-fit lines with equations shown along the curves. The circled data is an apparent outlier (see text).

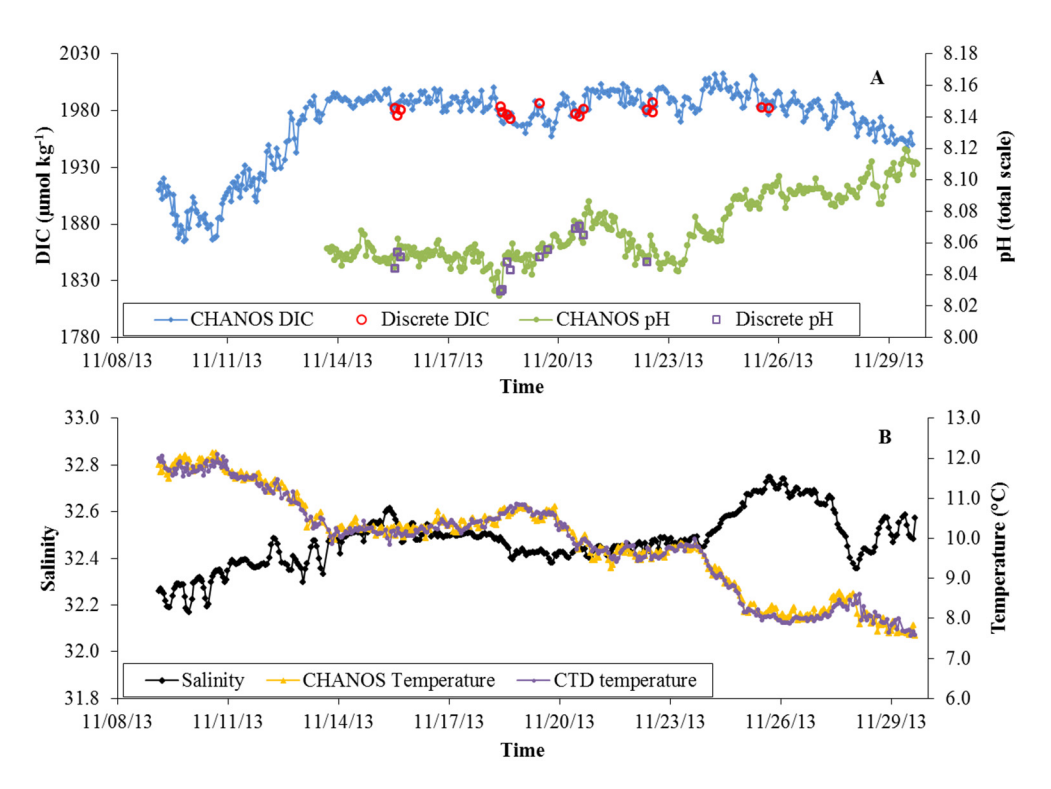


Figure 7. In-situ measurements of the CHANOS sensor along with discrete measurements at the WHOI Iselin dock: (A) CHANOS DIC and pH measurements along with discrete DIC and pH measurements; (B) Salinity and temperature. Salinity was measured by a SBE CTD Fastcat 49. Temperature was measured by both the CTD and a built-in thermistor in the CHANOS. The difference between the CTD and CHANOS temperature was  $-0.04\pm0.15^{\circ}$ C (n = 382). Each DIC and pH data point represents a mean of near continuous measurements taken over  $\sim$ 6 – 8 minutes (n = 30 – 40) in a measurement cycle.

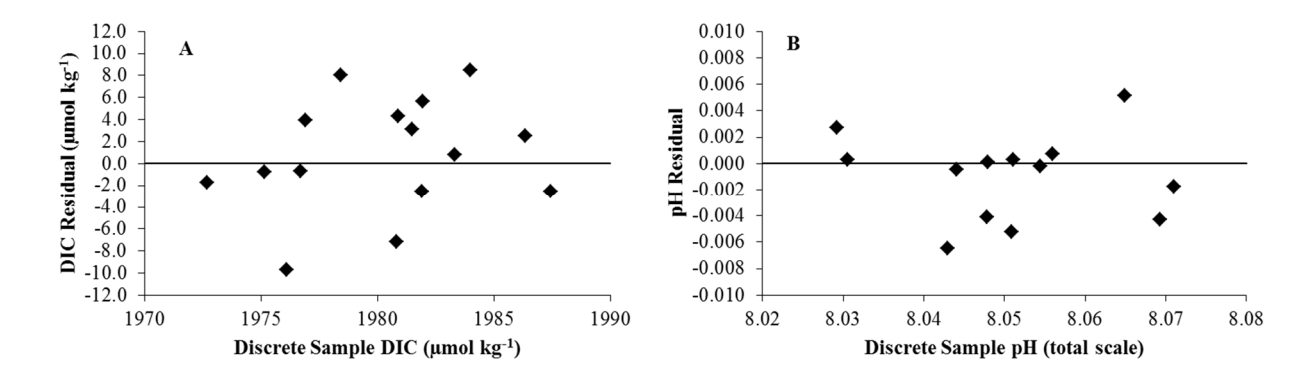


Figure 8. Residuals between the CHANOS sensor and bottle measurements over the range of sample DIC (A) and pH (B). Data from Figure 7.

## **AUTHOR INFORMATION**

## **Corresponding Author**

Zhaohui Aleck Wang; Email: zawang@whoi.edu; Telephone: 1-508-289-3676; Fax: 1-508-457-

#### **ACKNOWLEDGMENT**

This work was supported by WHOI Innovative Technology Award, National Institute of Standards and Technology (NIST-60NANB10D024), National Science Foundation (OCE-1233654 and OCE-1041068), and The Link Foundation Ocean Engineering and Instrumentation Ph.D. Fellowship. The authors would like to express gratitude to three anonymous reviewers for their insightful comments, which greatly improved the quality of the paper.

## **Supporting Information Available**

Supporting Information contains a comparison of three reported DIC in-situ sensors, details of CHANOS hardware, software, and measurement cycles, a description of discrete bottle

- 414 measurements, and evidence supporting the stability of CRM and indicator solution. This
- information is available free of charge via the Internet at http://pubs.acs.org/.
- 416
- 417

418 REFERENCE

- 420 1. Wanninkhof, R.; Park, G. H.; Takahashi, T.; Sweeney, C.; Feely, R.; Nojiri, Y.; Gruber,
- N.; Doney, S. C.; McKinley, G. A.; Lenton, A.; Le Quere, C.; Heinze, C.; Schwinger, J.; Graven,
- 422 H.; Khatiwala, S., Global ocean carbon uptake: magnitude, variability and trends.
- 423 *Biogeosciences* **2013**, *10* (3), 1983-2000.
- 424 2. Le Quere, C.; Takahashi, T.; Buitenhuis, E. T.; Rodenbeck, C.; Sutherland, S. C., Impact
- of climate change and variability on the global oceanic sink of CO<sub>2</sub>. Global Biogeochem. Cy.
- 426 **2010,** *24.* DOI: 10.1029/2009GB003599
- 3. Sabine, C. L.; Tanhua, T., Estimation of anthropogenic CO<sub>2</sub> inventories in the ocean.
- 428 Annu. Rev. Mar. Sci. 2010, 2, 175-198.
- 429 4. Doney, S. C.; Fabry, V. J.; Feely, R. A.; Kleypas, J. A., Ocean Acidification: The other
- 430 CO<sub>2</sub> problem. Annu. Rev. Mar. Sci. **2009**, 1, 169-192. DOI
- 431 10.1146/annurev.marine.010908.163834.
- 432 5. Feely, R. A.; Doney, S. C.; Cooley, S. R., Ocean Acidification: Present Conditions and
- Future Changes in a High-CO2 World. *Oceanography* **2009**, *22* (4), 36-47.
- 6. Orr, J. C.; Fabry, V. J.; Aumont, O.; Bopp, L.; Doney, S. C.; Feely, R. A.; Gnanadesikan,
- 435 A.; Gruber, N.; Ishida, A.; Joos, F.; Key, R. M.; Lindsay, K.; Maier-Reimer, E.; Matear, R.;
- 436 Monfray, P.; Mouchet, A.; Najjar, R. G.; Plattner, G. K.; Rodgers, K. B.; Sabine, C. L.;
- Sarmiento, J. L.; Schlitzer, R.; Slater, R. D.; Totterdell, I. J.; Weirig, M. F.; Yamanaka, Y.; Yool,
- 438 A., Anthropogenic ocean acidification over the twenty-first century and its impact on calcifying
- 439 organisms. *Nature* **2005**, *437* (7059), 681-686. Doi 10.1038/Nature04095.

- 440 7. Fabry, V. J.; Seibel, B. A.; Feely, R. A.; Orr, J. C., Impacts of ocean acidification on
- marine fauna and ecosystem processes. ICES J. Mar. Sci. 2008, 65 (3), 414-432.
- 442 8. Egleston, E. S.; Sabine, C. L.; Morel, F. M. M., Revelle revisited: Buffer factors that
- quantify the response of ocean chemistry to changes in DIC and alkalinity. Global Biogeochem.
- 444 *Cy.* **2010**, *24*. GB1002, doi:10.1029/2008GB003407.
- Byrne, R. H.; DeGrandpre, M. D.; Short, R. T.; Martz, T. R.; Merlivat, L.; McNeil, C.;
- Sayles, F.; Bell, R. A.; Fietzek, P. In Sensors and Systems for In Situ Observations of Marine
- 447 Carbon Dioxide System Variables, OceanObs'09, Venice, Italy, Sept. 21 25, 2009; Hall, J.;
- Harrison, D. E.; Stammer, D., Eds. ESA Publication WPP-306: Venice, Italy, 2010.
- 449 10. Feely, R. A.; Fabry, V. J.; Dickson, A. G.; Gattuso, J.-P.; Bijma, J.; Riebesell, U.; Doney,
- 450 S.; Turley, C.; Saino, T.; Lee, K.; Anthony, K.; Kleypas, J. In An international observational
- 451 network for ocean acidification, OceanObs'09: Sustained Ocean Observations and Information
- for Society, Venice, Italy, 21-25 September 2009; Hall, J.; Harrison, D. E.; Stammer, D., Eds.
- 453 ESA Publication WPP-306: Venice, Italy, 2010.
- 454 11. Johnson, K. S.; Berelson, W. M.; Boss, E. S.; Chase, Z.; Claustre, H.; Emerson, S. R.;
- 455 Gruber, N.; Kortzinger, A.; Perry, M. J.; Riser, S. C., Observing biogeochemical cycles at global
- scales with profiling floats and gliders prospects for a global array. Oceanography 2009, 22 (3),
- 457 216-225.
- 458 12. Moore, T. S.; Mullaugh, K. M.; Holyoke, R. R.; Madison, A. N. S.; Yucel, M.; Luther, G.
- W., Marine Chemical Technology and Sensors for Marine Waters: Potentials and Limits. *Annu.*
- 460 Rev. Mar. Sci. **2009**, 1, 91-115.
- 461 13. Prien, R. D., The future of chemical in situ sensors. *Mar. Chem.* **2007**, *107* (3), 422-432.

- 462 14. Johnson, K. S.; Needoba, J. A.; Riser, S. C.; Showers, W. J., Chemical sensor networks
- 463 for the aquatic environment. *Chem. Rev.* **2007**, *107* (2), 623-640.
- 15. Dickson, A. G.; Sabine, C. L.; Christian, J. R., Guide to best practices for ocean CO2
- 465 measurements. PICES Special Publication: Sidney, British Columbia, Canada, 2007; p 191.
- 466 16. Millero, F. J., The marine inorganic carbon cycle. *Chem. Rev.* **2007**, *107* (2), 308-341.
- 467 17. Martz, T. R.; Connery, J. G.; Johnson, K. S., Testing the Honeywell Durafet (R) for
- seawater pH applications. *Limnol Oceanogr-Meth* **2010**, *8*, 172-184.
- 469 18. Seidel, M. P.; DeGrandpre, M. D.; Dickson, A. G., A sensor for in situ indicator-based
- 470 measurements of seawater pH. Mar. Chem. 2008, 109 (1-2), 18-28. DOI
- 471 10.1016/j.marchem.2007.11.013.
- 472 19. Liu, X. W.; Wang, Z. H. A.; Byrne, R. H.; Kaltenbacher, E. A.; Bernstein, R. E.,
- 473 Spectrophotometric measurements of pH in-situ: Laboratory and field evaluations of
- 474 instrumental performance. *Environ. Sci. Technol.* **2006**, *40* (16), 5036-5044.
- Nakano, Y.; Kimoto, H.; Watanabe, S.; Harada, K.; Watanabe, Y. W., Simultaneous
- vertical measurements of in situ pH and CO<sub>2</sub> in the sea using spectrophotometric profilers. J.
- 477 Oceanogr. 2006, 62 (1), 71-81.
- 478 21. DeGrandpre, M. D.; Baehr, M. M.; Hammar, T. R., Calibration-free optical chemical
- 479 sensors. Anal. Chem. **1999**, 71 (6), 1152-1159.
- 480 22. Wang, Z. H. A.; Liu, X. W.; Byrne, R. H.; Wanninkhof, R.; Bernstein, R. E.;
- 481 Kaltenbacher, E. A.; Patten, J., Simultaneous spectrophotometric flow-through measurements of
- 482 pH, carbon dioxide fugacity, and total inorganic carbon in seawater. Anal. Chim. Acta 2007, 596
- 483 (1), 23-36.

- 23. Clayton, T. D.; Byrne, R. H., Spectrophotometric seawater pH measurements Total
- 485 hydrogen ion concentration scale calibration of *m*-cresol purple and at-sea results. *Deep-Sea Res*.
- 486 *(I)* **1993,** *40* (10), 2115-2129.
- 487 24. Liu, X.; Byrne, R. H.; Adornato, L.; Yates, K. K.; Kaltenbacher, E.; Ding, X.; Yang, B.,
- In situ spectrophotometric measurement of dissolved inorganic carbon in Seawater. *Environ. Sci.*
- 489 *Technol.* **2013,** 47 (19), 11106-11114. 10.1021/es4014807.
- 490 25. Sayles, F. L.; Eck, C., An autonomous instrument for time series analysis of TCO<sub>2</sub> from
- 491 oceanographic moorings. *Deep-Sea Res. (I)* **2009**, *56* (9), 1590-1603.
- 492 26. Byrne, R. H.; Liu, X. W.; Kaltenbacher, E. A.; Sell, K., Spectrophotometric measurement
- of total inorganic carbon in aqueous solutions using a liquid core waveguide. *Anal. Chim. Acta*
- 494 **2002,** *451* (2), 221-229.
- 495 27. Wang, Z. A.; Chu, S. N.; Hoering, K. A., High-frequency spectrophotometric
- 496 measurements of total dissolved inorganic carbon in seawater. Environ. Sci. Technol. 2013, 47
- 497 (14), 7840-7847.
- 28. Zhang, H. N.; Byrne, R. H., Spectrophotometric pH measurements of surface seawater at
- in-situ conditions: Absorbance and protonation behavior of thymol blue. Mar. Chem. 1996, 52
- 500 (1), 17-25.
- 501 29. Liu, X. W.; Patsavas, M. C.; Byrne, R. H., Purification and characterization of meta-
- cresol purple for spectrophotometric seawater pH measurements. Environ. Sci. Technol. 2011, 45
- 503 (11), 4862-4868. Doi 10.1021/Es200665d.
- 30. Bandstra, L.; Hales, B.; Takahashi, T., High-frequency measurements of total CO2:
- Method development and first oceanographic observations. *Mar. Chem.* **2006,** *100* (1-2), 24-38.

- 506 31. Piiper, J.; Scheid, P., Maximum gas transfer efficacy of models for fish gills, avian lungs
- and mammalian lungs. Resp. Physiol. 1972, 14 (1-2), 115-&.
- 508 32. Jurgens, K. D.; Gros, G., Phylogeny of gas exchange systems. Anasthesiologie
- 509 Intensivmedizin Notfallmedizin Schmerztherapie **2002**, *37* (4), 185-198.
- Weiss, R. F., Carbon dioxide in water and seawater: The solution of a non-ideal gas. *Mar*.
- 511 *Chem.* **1974,** *2*, 203-215.

- 512 34. Yao, W. S.; Byrne, R. H., Spectrophotometric determination of freshwater pH using
- bromocresol purple and phenol red. *Environ. Sci. Technol.* **2001,** *35* (6), 1197-1201.
- 514 35. Wang, Z. A.; Cai, W. J.; Wang, Y. C.; Upchurch, B. L., A long pathlength liquid-core
- waveguide sensor for real-time pCO(2) measurements at sea. Mar. Chem. 2003, 84 (1-2), 73-84.
- 516 36. Li, Q. L.; Wang, F. Z.; Wang, Z. A.; Yuan, D. X.; Dai, M. H.; Chen, J. S.; Dai, J. W.;
- Hoering, K. A., Automated spectrophotometric analyzer for rapid single-point titration of
- 518 seawater total alkalinity. *Environ. Sci. Technol.* **2013,** 47 (19), 11139-11146.